Spin Wave Analysis of Heisenberg Magnets in Restricted Geometries

[Lecture Notes in Physics v. 645, pp. 195-226 (2004)]

Nedko B. Ivanov[1] and Diptiman Sen[2]

[1] Theoretische Physik II, Universität Augsburg, D-86135 Augsburg, Germany**
ivanov@physik.uni-augsburg.de
[2] Center for Theoretical Studies, Indian Institute of Science, Bangalore 560012, India diptiman@cts.iisc.ernet.in

Summary. In the last decade it has been proven that the standard spin-wave theory was able to provide accurate zero-temperature results for a number of low-dimensional Heisenberg spin systems. In this chapter we introduce the main ingredients of the spin-wave technique using as a working model the two-leg mixed-spin ferrimagnetic ladder and the Dyson–Maleev boson formalism up to second order in the spin-wave interaction. In the remainder, we survey typical applications in low-space dimensionality as well as some recent modifications of the theory admitting a quantitative analysis in magnetically disordered phases. The presented spin-wave results are compared with available numerical estimates.

1 Introduction

The spin-wave theory is probably one of the most powerful tools ever used in the theory of magnetism. Originally proposed by Bloch [1, 2] and Holstein and Primakoff [3] as a theory of the ferromagnetic state, it was later extended for the antiferromagnetic Néel state by Anderson [4], Kubo [5], and Oguchi [6]. Dyson's profound analysis of spin-wave interactions [7, 8] demonstrated that spin waves may be used to obtain asymptotic expansions for the thermodynamic functions of the Heisenberg ferromagnet at low temperatures. Dyson's method was generalized by Harris et al. [9] to calculate in a systematic way spin-spin correlations, spin-wave damping, and various thermodynamic properties of antiferromagnetic insulators.

It should be noticed that the basis of the spin-wave theory (SWT) for antiferromagnets is much less established than for ferromagnets. The Dyson–Maleev transformation [10] gives a correspondence between any operator defined on the Hilbert space of the spin system and an operator on the boson Hilbert space. Evaluating the required averages for the Bose system, we necessarily make two approximations. First, we expand these quantities, by using a perturbation formalism in which the unperturbed Hamiltonian is quadratic in boson operators and the perturbation is the remaining quartic interaction. Second, we neglect the projection operator in the averages, which takes into account the so-called kinematic interactions by canceling the boson states with more than $2S$ bosons per lattice site, S being the spin quantum number of the lattice spin. In the ferromagnetic case, Dyson has argued that

** Permanent address: Institute of Solid State Physics, Bulgarian Academy of Sciences, Tsarigradsko chausse 72, 1784 Sofia, Bulgaria

these approximations would lead to results which are asymptotically correct at low temperatures (T) to all orders in T. In the antiferromagnetic case, the situation is less settled due to the zero-point motion, i.e. quantum spin fluctuations in the Néel state. In principle, one may suspect that there are errors in the perturbation theory even at zero T. The same problem appears in the Holstein–Primakoff formalism [3]. We refer the interested reader to the original papers cited above as well as to the monographs [11, 12, 13] for details concerning this problem. In principle, the spin-wave approach is less effective for low-dimensional quantum spin systems, as quantum spin fluctuations typically increase in reduced space dimensions (D) and for small spin quantum numbers S. Moreover, since at finite T thermal fluctuations completely destroy the magnetic long-range order in 1D and 2D Heisenberg models with isotropic short-range interactions [14], in such cases the conventional SWT completely fails.

In view of the mentioned drawbacks of SWT, it seems surprising that for the last decade the standard spin-wave approach has been found to give very accurate description of the zero-temperature physics of a number of low-dimensional spin models, the best example being the $S = \frac{1}{2}$ Heisenberg antiferromagnet on a square lattice [15]. Probably, another good example is the mixed-spin Heisenberg chain describing a large class of recently synthesized quasi-1D molecular magnets [16] (cf. Chap. 4). The following analysis reveals some common features of these examples, the most important being the weakness (in a sense) of spin-wave interactions. Fortunately, in low-space dimensions many numerical techniques – such as the quantum Monte Carlo method (QMC), the exact numerical diagonalization (ED), and the density-matrix renormalization group method (DMRG) – are more effective, so that the discussed drawbacks of the spin-wave analysis may be partially reduced by a direct combination with numerical methods.

A goal of the present review is to summarize typical applications and some recent developments of the spin-wave approach related to low-dimensional quantum spin systems. The spin-wave technique is presented in the following Sect., using the mixed-spin Heisenberg ladder as a working model and the Dyson–Maleev boson formalism. Due to the asymptotic character of spin-wave series, the calculation up to second order in the spin-wave interaction is a reasonable approximation for most of the applications at zero T. As far as at this level perturbative corrections can easily be calculated in the framework of the Rayleigh–Schrödinger theory, we will not consider in detail perturbation techniques based on magnon Green's functions [9, 17]. Typical applications of the spin-wave formalism in low-dimensional spin systems are presented in Sects. 3 and 4. In particular, Sect. 3 involves an analysis of the parameters of the quantum ferrimagnetic phase in mixed-spin quasi-1D models, such as the (s_1, s_2) Heisenberg chain. The SWT results are compared with available DMRG and ED numerical estimates. Section 4 collects basic SWT results concerning 2D Heisenberg antiferromagnets. Some recent modifications of the SWT – admitting a quantitative analysis in magnetically disordered phases – are presented in Sect. 5. Section 6 contains concluding remarks.

2 Dyson–Maleev Formalism

In this Sect. we describe the formal apparatus of the SWT. We choose as a working model the mixed-spin Heisenberg ladder (Fig. 1) defined by the Hamiltonian

$$\mathcal{H} = \sum_{n=1}^{N} [\boldsymbol{s}_n \cdot \boldsymbol{\sigma}_{n+1} + \boldsymbol{\sigma}_n \cdot \boldsymbol{s}_{n+1}] + J_\perp \sum_{n=1}^{N} \boldsymbol{s}_n \cdot \boldsymbol{\sigma}_n \,, \tag{1}$$

where the index n $(= 1, \cdots, N)$ labels the rungs of the ladder, and N is an even integer. The ladder is composed of two types of spins $(\boldsymbol{s_n}, \boldsymbol{\sigma_n})$ characterized by the spin quantum numbers s_1 and s_2 $(s_1 > s_2)$: $\boldsymbol{s_n}^2 = \hbar^2 s_1(s_1+1)$ and $\boldsymbol{\sigma_n}^2 = \hbar^2 s_2(s_2+1)$. In the following text we use the notation $r_s \equiv s_1/s_2 > 1$, and set $\hbar = 1$ and $a_0 = 1$, a_0 being the lattice spacing along the ladder.

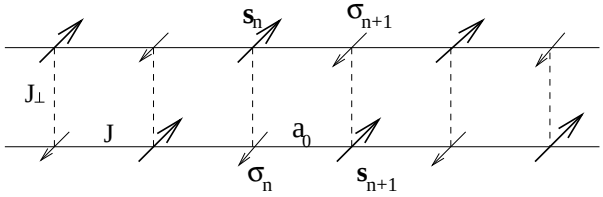

Fig. 1. Mixed-spin Heisenberg ladder composed of two types of site spins. The arrows show one of the classical ground states for $J_\perp > 0$, defined by the orientation of the ferromagnetic moment $\boldsymbol{M} = \sum_{n=1}^{N} (\boldsymbol{s}_n + \boldsymbol{\sigma}_n)$. The intrachain coupling $J = 1$.

It is worth noticing that the model (1) is not purely academic. For instance, recently published experimental work on bimetallic quasi-1D molecular magnets (cf. Chap. 4) implies that the magnetic properties of these mixed-spin compounds are basically described by the Heisenberg spin model with antiferromagnetically coupled nearest-neighbor localized spins. The ladder structure in Fig. 1 reproduces, in particular, arrangements of the Mn $(s_1 = \frac{5}{2})$ and the Cu $(s_2 = \frac{1}{2})$ magnetic atoms along the a axis in the compounds $MnCu(pbaOH)(H_2O)_3$ (pbaOH = 2–hydroxy–1,3–propylenebisoxamato) [18].

2.1 Classical Reference State

The first step in constructing a spin-wave expansion is to find the lowest-energy classical spin configurations of the related classical model. As a rule, this is a straightforward task, apart from some magnetic models with competing interactions which may exhibit complicated non-collinear spin states (see, e.g. [19]). Another serious problem at this stage may be related to a macroscopic degeneracy of the classical ground state, a typical example being the Heisenberg model on a kagomé lattice (cf. Chap. 3) which exhibits a magnetically disordered ground state. Further analysis of the problem involves quantum fluctuations and the so-called *order-from-disorder phenomenon* [20, 21].

Turning to our model (1), it is easy to see that the required reference state for $J_\perp > 0$ is a ferrimagnetic spin configuration where the $\boldsymbol{s}_n$ spins are oriented in a given direction, and the $\boldsymbol{\sigma}_n$ spins point in the opposite direction (see Fig. 1). The state is degenerate under arbitrary rotations (as a whole) in the spin space. One may pick up a reference state by introducing a small staggered field, say, for the $\boldsymbol{s}_n$ spins. We can actually get more information even in the quantum case, by

using the Lieb–Mattis theorem for bipartite lattices [22]. First, the theorem predicts that the quantum ground state belongs to a subspace with the total-spin quantum number $(S_1 - S_2)N$, i.e. for $J_\perp > 0$ the system has a ferrimagnetic ground state characterized by the ferromagnetic moment per site $M_0 = (s_1 - s_2)/2$. Second, the theorem states that the energies of the ground states $E(S_T)$ characterized by the total-spin quantum numbers $S_T \geq N(s_1 - s_2)$ are arranged as follows

$$E(S_T + 1) > E(S_T)\,. \tag{2}$$

Notice that the classical and quantum ferrimagnetic ground states have one and the same magnetization M_0, but otherwise they are different because the classical ground state is not an eigenstate of the quantum model (1). The quantum ferrimagnetic state is $[2N(s_1 - s_2) + 1]$-fold degenerate, since the z component of the total spin – being a good quantum number – takes the values $-N(s_1 - s_2), -N(s_1 - s_2) + 1, \cdots, N(s_1 - s_2)$. This quantum magnetic phase may also be characterized by the following sublattice magnetizations

$$\boldsymbol{m}_A = \frac{1}{N}\sum_{n=1}^{N}\langle \boldsymbol{s}_n \rangle \quad \boldsymbol{m}_B = \frac{1}{N}\sum_{n=1}^{N}\langle \boldsymbol{\sigma}_n \rangle\,, \tag{3}$$

where the symbol $\langle \cdots \rangle$ means a quantum-mechanical average over the ground state. We shall later see that quantum spin fluctuations reduce the classical sublattice magnetizations s_1 and s_2, but the magnetic long-range order is preserved, i.e. $\boldsymbol{m}_A, \boldsymbol{m}_B \neq 0$.

In the region $J_\perp < 0$ the situation is different, i.e. the lowest-energy spin configuration is the Néel antiferromagnetic state based on the composite rung spins $s_1 + s_2$. Now the Lieb–Mattis theorem predicts that the exact quantum ground state is a spin-singlet state, i.e. $S_T = 0$ and $M_0 = 0$. Therefore, it may be generally expected a magnetically disordered phase, t.e. $\boldsymbol{m}_A, \boldsymbol{m}_B = 0$, as the isotropic Heisenberg model (1) is defined on a bipartite 1D lattice (see, e.g. [23]). In terms of the SWT this would mean that the classical antiferromagnetic state is swept out by quantum fluctuations, so that the concept of the spin-wave expansion does not work at all.

2.2 Boson Hamiltonian

Now we describe the second step in constructing the spin-wave expansion, t.e. the transformation of (1) to a boson Hamiltonian. The most popular boson representation of spin operators has been suggested by Holstein and Primakoff [3]. Other useful representations have been devised by Schwinger [24], Maleev [10], Villain [25], and Goldhirsch [26, 27].

We start by defining the Holstein–Primakoff representation for the spins $\boldsymbol{s}_n$ $(n = 1, \ldots, N)$:

$$s_n^+ = \sqrt{2s_1}\,\sqrt{1 - \frac{a_n^\dagger a_n}{2s_1}}\;a_n\,,\;\; s_n^- = \sqrt{2s_1}\,a_n^\dagger\sqrt{1 - \frac{a_n^\dagger a_n}{2s_1}}\,,\;\; s_n^z = s_1 - a_n^\dagger a_n\,, \tag{4}$$

where $s_n^\pm = s_n^x \pm s_n^y$ and s_1 is the spin quantum number. a_n and $a_n^\dagger$ are annihilation and creation boson operators satisfying the commutation relations

$$[a_n, a_m^\dagger] = \delta_{nm}, \quad [a_n, a_m] = [a_n^\dagger, a_m^\dagger] = 0\,. \tag{5}$$

Using the last equations, it is easy to show that the operators defined by (4) satisfy the commutation relations for spin operators

$$[s_n^+, s_n^-] = 2s_n^z\,, \qquad [s_n^z, s_n^\pm] = \pm s_n^\pm\,, \tag{6}$$

and the equation $\boldsymbol{s}_n^2 = s_1(s_1+1)$. The operators a_n and $a_n^\dagger$ act in the infinite-dimensional boson Hilbert space spanned by the orthonormal basis states

$$|n_1, n_2, \ldots, n_N) = \frac{(a_1^\dagger)^{n_1}(a_2^\dagger)^{n_2}\cdots(a_N^\dagger)^{n_N}}{\sqrt{n_1!n_2!\ldots n_N!}}|0)\,, \tag{7}$$

where n_i $(= 0, 1, \ldots, \infty)$ is the occupation number of site i. The reference vacuum state $|0)$ is defined by the relations $a_i|0) = 0$ (for $\forall\ i$).

It is possible to rationalize the square roots in (4) by the Maleev similarity transformation

$$a_n \longmapsto \left(1 - \frac{a_n^\dagger a_n}{2s_1}\right)^{1/2} a_n\,, \qquad a_n^\dagger \longmapsto a_n^\dagger \left(1 - \frac{a_n^\dagger a_n}{2s_1}\right)^{-1/2}. \tag{8}$$

This transformation is not unitary, but preserves the number operator $a_n^\dagger a_n$ as well as the commutation relations (5) within the physically relevant Hilbert space ($n_i \le 2s_1$ for $\forall\, i$). Applying the last transformation to (4), we get the Dyson–Maleev boson representation

$$s_n^+ = \sqrt{2s_1}\,(1 - a_n^\dagger a_n/2s_1)\,a_n\,, \qquad s_n^- = \sqrt{2s_1}\,a_n^\dagger\,, \qquad s_n^z = s_1 - a_n^\dagger a_n\,. \tag{9}$$

Note that the operators $s_n^\pm$ in this representation are not Hermitian conjugate in the boson space (7) so that in the general case they will generate non-Hermitian Hamiltonians. Treatment of such Hamiltonians requires some care, but it seems that – at least up to second order in the spin-wave interaction – this does not cause serious problems. More problematic is the relation between physical and unphysical states. The latter appear in the exact Holstein–Primakoff representation as well, as any actual calculation requires truncation of the asymptotic square-root series. Dyson's method [7] eliminates the unphysical boson states by a projection operator giving zero on these states. In practice, however, we are enforced to eliminate this operator. As already mentioned, this is the basic approximation of SWT. As a whole, the Dyson–Maleev formalism has many advantages if one needs to go beyond the linear spin-wave theory (LSWT) within a perturbation scheme. This is because the interactions between spin waves are better handled so that the unphysical singularities caused by the long-wavelength spin waves cancel out.

To continue, we write a representation similar to (9) for the spins $\boldsymbol{\sigma}_n$, by using a new set of boson fields (b_n, $n = 1, \ldots, N$):

$$\sigma_n^+ = \sqrt{2s_2}\,b_n^\dagger\,(1 - b_n^\dagger b_n/2s_2)\,, \qquad \sigma_n^- = \sqrt{2s_2}\,b_n\,, \qquad \sigma_n^z = -s_2 + b_n^\dagger b_n\,. \tag{10}$$

b_n and $b_n^\dagger$ satisfy the same commutation relations (5), and are supposed to commute with the set of a bosons. Here the reference state is chosen in the opposite direction, in accord with the classical spin configuration in Fig. 1.

Using (9) and (10), we can find the boson image of any function of spin operators. In particular, we are interested in the boson representation of the spin

Hamiltonian (1), which we denote by $\mathcal{H}_B$. For the purposes of SWT, it is instructive to express $\mathcal{H}_B$ in terms of the Fourier transforms a_k and b_k of the boson operators a_n and b_n, by using the unitary Fourier transformations

$$a_n = \frac{1}{\sqrt{N}} \sum_k \mathrm{e}^{\mathrm{i}kn} a_k \,, \qquad b_n = \frac{1}{\sqrt{N}} \sum_k \mathrm{e}^{-\mathrm{i}kn} b_k \,, \tag{11}$$

and the identity

$$\frac{1}{N} \sum_{n=1}^{N} \mathrm{e}^{\mathrm{i}(k-k')n} = \delta_{kk'} \,.$$

It may be verified that this transformation is canonical, by showing that the new operators a_k and b_k obey a set of commutation relations identical to (5). The wave vectors k in the last expressions are defined in the first Brillouin zone:

$$k = \frac{2\pi}{N} l \,, \qquad l = -\frac{N}{2}+1, -\frac{N}{2}+2, \ldots, \frac{N}{2}, \ .$$

Notice that the rung spins $(\boldsymbol{s}_n, \boldsymbol{\sigma}_n)$ in Fig. 1 compose the n-th magnetic (and lattice) elementary cell: this may be easily observed by interchanging the site spins of every (say) even rung in Fig. 1.

We leave the Fourier transformation of $\mathcal{H}_B$ as an exercise, and directly present the result in terms of the new operators a_k and b_k:

$$\mathcal{H}_B = -2\gamma_0 r_s S^2 + \mathcal{H}_0 + V_{DM}^{'} \,, \tag{12}$$

where

$$\mathcal{H}_0 = 2S \sum_k \left[\gamma_0 \left(a_k^\dagger a_k + r_s b_k^\dagger b_k \right) + \sqrt{r_s} \gamma_k \left(a_k^\dagger b_k^\dagger + a_k b_k \right) \right] \,, \tag{13}$$

$$V_{DM}^{'} = -\frac{1}{N} \sum_{1-4} \delta_{12}^{34} \left(2\gamma_{1-4} a_3^\dagger a_2 b_1^\dagger b_4 + \sqrt{r_s} \gamma_{1+2-4} a_3^\dagger b_2^\dagger b_1^\dagger b_4 + \frac{1}{\sqrt{r_s}} \gamma_4 a_3^\dagger a_2 a_1 b_4 \right) . \tag{14}$$

Here $\gamma_k = J_\perp/2 + \cos k$ ($\gamma_0 = J_\perp/2 + 1$), $\delta_{12}^{34} \equiv \Delta(k_1 + k_2 - k_3 - k_4)$ is the *Kronecker function*, and we have introduced the abbreviations $(k_1, k_2, k_3, k_4) \equiv (1, 2, 3, 4)$ for the wave vectors.

In a standard spin-wave expansion, $1/s_1$ and $1/s_2$ are treated as small parameters, whereas the parameter r_s may be considered as a fixed number of order unity. In such a perturbation scheme, it is convenient to set $1/S \equiv 1/s_2$ and use $1/S$ as a small parameter. Thus, the first term in (12) – the classical ground-state energy – is proportional to S^2, the LSWT Hamiltonian $\mathcal{H}_0$ is multiplied by S, and the spin-wave interaction term $V_{DM}^{'}$ has the order $\mathcal{O}(1)$. We shall follow a perturbation scheme where the diagonal terms of $V_{DM}^{'}$, i.e. terms proportional to the occupation-number operators $a_k^\dagger a_k$ and $b_k^\dagger b_k$, are treated together with $\mathcal{H}_0$ as a zeroth-order Hamiltonian, whereas the rest of $V_{DM}^{'}$ is taken as a perturbation [9]. This is a more generic approach because for some reasons the spin-wave interactions may be weak even in the extreme quantum systems with $1/S = 2$.

2.3 Quasiparticle Representation

In the next step, we diagonalize the quadratic Hamiltonian $\mathcal{H}_0$, by using the Bogoliubov canonical transformation to quasiparticle boson operators (α_k and β_k) [3]:

$$a_k = u_k(\alpha_k - x_k\beta_k^\dagger)\,, \quad b_k = u_k(\beta_k - x_k\alpha_k^\dagger)\,, \quad u_k^2(1-x_k^2) = 1\,. \tag{15}$$

It is a simple exercise to find the transformation parameters u_k and x_k from the condition which eliminates the off-diagonal terms $\alpha_k\beta_k$ appearing in $\mathcal{H}_0$ after the transformation (15). The result reads

$$u_k = \sqrt{\frac{1+\varepsilon_k}{2\varepsilon_k}}\,, \quad x_k = \frac{\eta_k}{1+\varepsilon_k}\,, \tag{16}$$

where

$$\varepsilon_k = \sqrt{1-\eta_k^2}\,, \quad \eta_k = \frac{2\sqrt{r_s}}{r_s+1}\frac{\gamma_k}{\gamma_0}\,. \tag{17}$$

In some applications, the quadratic Hamiltonian $\mathcal{H}_0$ may include additional ferromagnetic bilinear terms (such as $a_k^\dagger b_k$) so that the actual diagonalization is more involved due to the increased number of parameters (16). Some diagonalization techniques for systems with large number of boson operators are presented in [11, 28].

A quasiparticle representation of the quartic terms (14) requires more technical work. As mentioned above, it is instructive to pick up the quadratic diagonal terms in $V_{DM}^{'}$ and to treat them together with $\mathcal{H}_0$ as a zeroth-order approximation. A simple way to do this is based on the presentation of $V_{DM}^{'}$ as a sum of normal-ordered products of boson quasiparticle operators. Apart from a constant, the resulting expression for $V_{DM}^{'}$ contains diagonal and off-diagonal quadratic operator terms, and normal-ordered quartic operator terms. We leave as an exercise this simple but somewhat cumbersome procedure and give the final result for $\mathcal{H}_B$ expressed in terms of the quasiparticle boson operators α_k and β_k:

$$\mathcal{H}_B = E_0 + \mathcal{H}_D + \lambda V\,, \qquad V = V_2 + V_{DM}\,, \qquad \lambda \equiv 1\,. \tag{18}$$

Here E_0 is the ground-state energy of the ferrimagnetic state calculated up to the order $\mathcal{O}(1)$ in the standard $1/S$ expansion:

$$\frac{E_0}{N} = -2\gamma_0 r_s S^2 - \gamma_0(1+r_s)\left(1 - \frac{1}{N}\sum_k \varepsilon_k\right)S + \mathrm{e}_1 + \mathcal{O}\left(\frac{1}{S}\right)\,, \tag{19}$$

where $\mathrm{e}_1 = -2(c_1^2+c_2^2) - J_\perp(c_1^2+c_3^2) - (2c_2 + J_\perp c_3)c_1(r_s+1)r_s^{-1/2}$ and

$$c_1 = -\frac{1}{2} + \frac{1}{2N}\sum_k \frac{1}{\varepsilon_k}\,, \quad c_2 = -\frac{1}{2N}\sum_k \cos k\frac{\eta_k}{\varepsilon_k}\,, \quad c_3 = -\frac{1}{2N}\sum_k \frac{\eta_k}{\varepsilon_k}\,. \tag{20}$$

$\mathcal{H}_D$ is the quadratic Hamiltonian resulting from $\mathcal{H}_0$ and the diagonal terms picked up from (14):

$$\mathcal{H}_D = 2S\sum_k \left[\omega_k^{(\alpha)}\alpha_k^\dagger\alpha_k + \omega_k^{(\beta)}\beta_k^\dagger\beta_k\right]\,, \tag{21}$$

where up to $\mathcal{O}\,(1/S)$ the *dressed dispersions* read

$$\omega_k^{(\alpha,\beta)} = \gamma_0 \left(\frac{r_s+1}{2} \varepsilon_k \mp \frac{r_s-1}{2} \right) + \frac{g_k^{\pm}}{2S} + \mathcal{O}\left(\frac{1}{S^2}\right) \tag{22}$$

where $g_k^{\pm} = (g_k \eta_k - d_0)\varepsilon_k^{-1/2}/2 \pm (r_s-1)(2c_2 + c_3 J_\perp) r_s^{-1/2}/2$, $g_k = 2c_1(r_s+1)\gamma_k r_s^{-1/2} + 4c_2 \cos k + 2c_3 J_\perp$, $d_0 = 4c_1\gamma_0 + (r_s+1)(2c_2 + J_\perp c_3) r_s^{-1/2}$.

The functions $\omega_k^{(\alpha,\beta)}$ without $\mathcal{O}(1/S)$ corrections will be referred to as *bare dispersions*.

Finally, the quasiparticle interaction V includes two different terms, i.e. the two-boson interaction

$$V_2 = \sum_k \left[V_k^+ \alpha_k^\dagger \beta_k^\dagger + V_k^- \alpha_k \beta_k \right] \tag{23}$$

defined by the vertex functions

$$V_k^{\pm} = \frac{d_0 \eta_k - g_k}{2\varepsilon_k} \mp \frac{r_s - 1}{\sqrt{r_s}} c_1 \gamma_k \,, \tag{24}$$

and the quartic Dyson–Maleev interaction

$$\begin{aligned} V_{DM} = -\frac{J}{2N} \sum_{1-4} \delta_{12}^{34} \Big[& V_{12;34}^{(1)} \alpha_1^\dagger \alpha_2^\dagger \alpha_3 \alpha_4 + 2 V_{12;34}^{(2)} \alpha_1^\dagger \beta_2 \alpha_3 \alpha_4 + 2 V_{12;34}^{(3)} \alpha_1^\dagger \alpha_2^\dagger \beta_3^\dagger \alpha_4 \\ & + 4 V_{12;34}^{(4)} \alpha_1^\dagger \alpha_3 \beta_4^\dagger \beta_2 + 2 V_{12;34}^{(5)} \beta_4^\dagger \alpha_3 \beta_2 \beta_1 + 2 V_{12;34}^{(6)} \beta_4^\dagger \beta_3^\dagger \alpha_2^\dagger \beta_1 \\ & + V_{12;34}^{(7)} \alpha_1^\dagger \alpha_2^\dagger \beta_3^\dagger \beta_4^\dagger + V_{12;34}^{(8)} \beta_1 \beta_2 \alpha_3 \alpha_4 + V_{12;34}^{(9)} \beta_4^\dagger \beta_3^\dagger \beta_2 \beta_1 \Big] \,, \end{aligned} \tag{25}$$

defined by the vertex functions $V_{12;34}^{(i)}$, $i = 1, \ldots, 9$. We have adopted the symmetric form of vertex functions used in [17]. The explicit form of $V_{12;34}^{(i)}$ depends on the concrete model. For the ladder model (1), the vertex functions may be obtained from those of the Heisenberg ferrimagnetic chain [29], using the formal substitution $\cos k \longmapsto \cos k + J_\perp/2$.

In the following we shall treat the spin-wave interaction V as a small perturbation to the diagonal Hamiltonian $E_0 + H_D$. To restore the standard $1/S$ series, one should (i) use bare dispersion functions, and (ii) resume the series in powers of $1/S$.

3 Spin Wave Analysis of Quasi-1D Ferrimagnets

In this Sect. we analyze the magnon spectrum and basic parameters of the quantum ferrimagnetic phase of the model (1), by using the developed spin-wave formalism and the Rayleigh–Schrödinger perturbation theory up to second order in λ. The SWT results are compared with available DMRG and ED numerical estimates.

3.1 Linear Spin Wave Approximations

In a standard linear spin-wave approximation we consider only the first two terms in (12), and discard $V_{DM}^{'}$ as a next-order term in $1/S$. This corresponds to the first two terms in the expression for the ground-state energy (19), and to the first term in the expression for the quasiparticle dispersions (22). As a matter of fact, by using the normal-ordering procedure, we have already got even the next-order terms of the expansions in $1/S$ for these quantities.

Magnon Excitation Spectrum

The quadratic Hamiltonian $\mathcal{H}_D$ defines two branches of spin-wave excitations (α and β magnons) described by the dispersion functions $\omega_k^{(\alpha,\beta)}$ in the first Brillouin zone $-\pi \leq k \leq \pi$ (see Fig. 2). The excited states $\alpha_k^\dagger|0\rangle$ ($\beta_k^\dagger|0\rangle$) belong to the subspace characterized by the quantum number $S_T^z = S_T - 1$ ($S_T^z = S_T + 1$), where $S_T = (s_1 - s_2)N$. In the long wavelength limit $k \ll 1$, the energies of α magnons $E_k^{(\alpha)}$ have the Landau–Lifshitz form

$$E_k^{(\alpha)} \equiv 2S\omega_k^{(\alpha)} = \frac{\varrho_s}{M_0}k^2 + \mathcal{O}(k^4)\,, \tag{26}$$

where ϱ_s is the spin stiffness constant [30]. This form of the Goldstone modes is typical for Heisenberg ferromagnets, and reflects the fact that the order parameter, i.e. the ferromagnetic moment, is itself a constant of the motion.

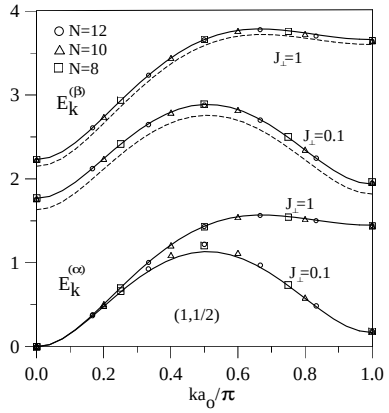

Fig. 2. Magnon excitation spectrum of the mixed-spin ladder $(s_1, s_2) = (1, \frac{1}{2})$ for interchain couplings $J_\perp = 0.1$ and $J_\perp = 1$. The dashed lines display the energy of β magnons $E_k^{(\beta)}$ related to the Hamiltonian $\mathcal{H}_D$. The solid lines show the magnon spectra as obtained from the second-order approximation in V. The energy of α magnons related to (22) is not displayed, as it closely follows the respective solid lines. The symbols indicate ED numerical results. The Figure is taken from [31].

The spin stiffness constant ϱ_s as well as M_0 play a basic role in the low-temperature thermodynamics [32]. The parameter ϱ_s may be obtained from the Landau–Lifshitz relation and (22):

$$\frac{\varrho_s}{2s_1 s_2} = 1 - \frac{1}{S}\left(c_1\frac{r_s+1}{r_s} + \frac{c_2}{\sqrt{r_s}}\right) + \mathcal{O}\left(\frac{1}{S^2}\right)\,. \tag{27}$$

The function $E_k^{(\alpha)}$ exhibits an additional minimum at the zone boundary, so that in the vicinity of π it reads

$$E_k^{(\alpha)} = \Delta_\pi^{(\alpha)} + \text{const}\,(\pi - k)^2\,. \tag{28}$$

Here $\Delta_\pi^{(\alpha)}$ is the excitation gap at the zone boundary. In the limit $J_\perp \to 0$, the excitation gap $\Delta_\pi^{(\alpha)}$ ($\propto J_\perp$) goes to zero. For ferromagnetic couplings $J_\perp < 0$, the $k = \pi$ mode becomes unstable and produces global instability of the ferrimagnetic phase.

The function $E_k^{(\beta)} \equiv 2S\omega_k^{(\beta)}$ may be characterized by the spectral gaps $\Delta_0^{(\beta)}$ (at $k = 0$) and $\Delta_\pi^{(\beta)}$ (at $k = \pi$). The expression for $\Delta_0^{(\beta)}$ reads

$$\Delta_0^{(\beta)} = 2\gamma_0(s_1 - s_2)\left(1 - \frac{2c_2 + c3J_\perp}{2S\gamma_0\sqrt{r_s}}\right) + \mathcal{O}\left(\frac{1}{S}\right). \tag{29}$$

For the $(s_1, s_2) = (1, \frac{1}{2})$ chain ($J_\perp = 0$), the last equations give the results $\varrho_s/2s_1s_2 = 0.761$ and $\Delta_0^{(\beta)} = 1.676$, to be compared with the results $\varrho_s/2s_1s_2 = 1$ and $\Delta_0^{(\beta)} = 1$ obtained in a standard linear approximation using the Hamiltonian $\mathcal{H}_0$ [33, 34]. A comparison with the numerical QMC result $\Delta_0^{(\beta)} = 1.759$ [35] clearly demonstrates the importance of the $1/S$ corrections to the dispersion functions (22) in the extreme quantum limit.

Summarizing, it may be stated that the linear approximation – based on the quadratic Hamiltonian $\mathcal{H}_D$ – gives a good qualitative description of the magnon excitation spectrum of the model (1). The same conclusion is valid for the ground-state energy: The expression (19) has been found to produce an excellent fit to the numerical ED results in a large interval up to $J_\perp = 10$ [31].

Sublattice Magnetizations

The on-site magnetizations $m_A = \langle s_n^z \rangle$ and $m_B = -\langle \sigma_n^z \rangle$ are parameters of the quantum ferrimagnetic phase which keep information for the long-range spin correlations. The simple LSWT results $m_A = s_1 - c_1$ and $m_B = s_2 - c_1$ show that quantum spin fluctuations reduce the classical on-site magnetizations already at the level of non-interacting spin waves. $\mathcal{H}_0$ produces the same results. The ratio

$$\frac{s_2 - m_B}{s_2} = \frac{c_1}{S} \tag{30}$$

may be used as a measure of the zero-point motion in the quantum ground state. Thus, there appears to be a well-defined semiclassical limit $S \to \infty$ where $\mathcal{H}_0$ is a sufficiently accurate approximation, provided $c_1/S \ll 1$. In this connection, it seems surprising that the spin-wave series for the $S = \frac{1}{2}$ square-lattice Heisenberg antiferromagnet produces the excellent result $m_A = 0.3069(2)$ [36] – the recent stochastic-series QMC estimate is 0.3070(3) [37] – in spite of the fact that in this case the parameter $c_1/S \approx 0.393$ is not small. Even more illuminating is the $(1, \frac{1}{2})$ ferrimagnetic chain: In spite of the large parameter $c_1/S \approx 0.610$, the second-order SWT gives the precise result $m_A = 0.79388$ [38] (DMRG estimate is $m_A = 0.79248$ [39]). It is difficult to explain the accuracy of SWT in terms of the standard $1/S$ series. However, as will be shown below, the quasiparticle interaction V produces numerically small corrections to the principal zeroth-order approximation.

In the mixed-spin model (1) there appears an important first-order correction to the sublattice magnetizations which is connected to the quadratic interaction V_2. Let us go beyond the linear approximation and calculate the $\mathcal{O}(\lambda)$ correction to m_A. The on-site magnetization m_B may be obtained from the exact relation

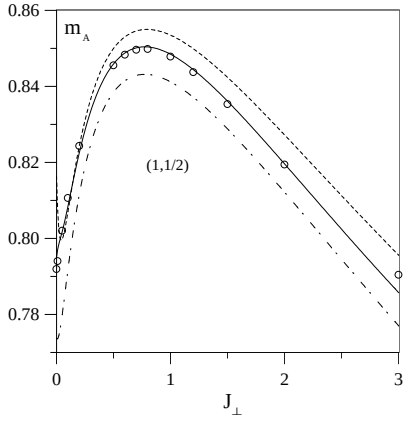

Fig. 3. On-site magnetization (sublattice $\mathcal{A}$) of the $(1, \frac{1}{2})$ ladder as a function of the interchain coupling $J_\perp$. The dashed and dashed-dotted lines display the series results up to first order in $1/S$ (bare dispersions) and V (dressed dispersions). The solid line shows the series result up to second order in V. The Lanczos ED results for ladders with $N = 12$ rungs are denoted by open circles. The Figure is taken from [31].

$m_A = s_1 - s_2 + m_B$ resulting from the conservation law for the ferromagnetic moment. The expression of m_A in terms of quasiparticle operators reads

$$m_A = s_1 - c_1 - \frac{1}{2N} \sum_k \left[\frac{1}{\varepsilon_k} \langle \alpha_k^\dagger \alpha_k + \beta_k^\dagger \beta_k \rangle - \frac{\eta_k}{\varepsilon_k} \langle \alpha_k^\dagger \alpha_k^\dagger + \beta_k^\dagger \beta_k^\dagger \rangle \right] . \qquad (31)$$

Now we make use of the standard perturbation formula

$$\langle \hat{O} \rangle^{(1)} = \sum_{n \neq 0} \frac{\langle 0|V|n\rangle \langle n|\hat{O}|0\rangle}{E_0 - E_n} + \sum_{n \neq 0} \frac{\langle n|V|0\rangle \langle 0|\hat{O}|n\rangle}{E_0 - E_n} \qquad (32)$$

giving the first-order correction in V of $\langle \hat{O} \rangle$. Here $\hat{O}$ is an arbitrary operator and $\langle \cdots \rangle$ means a quantum-mechanical average over the exact ground state. The formula is also valid in the case of non-Hermitian perturbations V. In our case, $\hat{O}$ is a quadratic operator, so that the sum in (32) is restricted to the two-boson eigenstates $|n_k\rangle = \alpha_k^\dagger \beta_k^\dagger |0\rangle$ of $\mathcal{H}_D$, k being a wave vector from the first Brillouin zone. The energies of these states are $E_k - E_0 = 2S(\omega_k^{(\alpha)} + \omega_k^{(\beta)})$. Finally, using the matrix elements

$$\langle 0|V_2|n_k\rangle = V_k^{(-)} , \qquad \langle n_k|V_2|0\rangle = V_k^{(+)} , \qquad (33)$$

we get the following result for m_A calculated up to first order in V:

$$m_A = s_1 - c_1 - \frac{1}{4SN} \sum_k \frac{\eta_k}{\varepsilon_k} \frac{V_k^{(+)} + V_k^{(-)}}{\omega_k^{(\alpha)} + \omega_k^{(\beta)}} + \mathcal{O}(\lambda^2) . \qquad (34)$$

To find the standard $1/S$ correction to m_A, we have to use in (34) the bare dispersion functions.

Figure 3 shows the results for m_A, as obtained from (34) by using the bare and dressed dispersion functions (22). It is seen that the expansion in $1/S$ gives a small (unexpected) decrease of m_A in the vicinity of $J_\perp = 0$, whereas the expansion in V produces a correct qualitative result in this limit. The indicated problem of the standard $1/S$ series probably results from enhanced fluctuations of the individual chain magnetizations about the common quantization axis. Indeed, at the special point $J_\perp = 0$ the classical ground state acquires an additional degeneracy under independent rotations of the chain ferromagnetic moments. Thus, the quartic diagonal interaction – included in $\mathcal{H}_D$ – seems to stabilize the common quantization axis connected to the global ferromagnetic moment. We have an example where the expansion in powers of V gives better results.

Antiferromagnetic Chain

It is instructive to consider the antiferromagnetic chain as a special case ($s_1 = s_2, J_\perp = 0$) of the mixed-spin model (1). After some algebra, from (19) and (22) we find the following simplified expressions for the ground-state energy (per site)

$$e_0 = -S^2 \left[1 + \frac{1}{2S}\left(1 - \frac{2}{\pi}\right)\right]^2 + \mathcal{O}\left(\frac{1}{S}\right) \tag{35}$$

and the magnon spectrum

$$\omega_k^{(\alpha,\beta)} \equiv \frac{E_k}{2S} = \left[1 + \frac{1}{2S}\left(1 - \frac{2}{\pi}\right)\right] |\sin k| + \mathcal{O}\left(\frac{1}{S^2}\right) \tag{36}$$

of the antiferromagnetic chain. For $S = \frac{1}{2}$, the standard LSWT gives the result $e_0 = -0.4317$ which is close to Hulthen's exact result $-\ln 2 + 1/4 \approx -0.443147$ [40]. It is an illuminating agreement, as the theory might have been expected to fail for magnetically disordered states. Notice, however, that the next-order approximation, i.e. $e_0 = -0.4647$, does not improve the SWT result. This indicates a poor convergence of the $1/S$ expansion. We can also check the series for $S = \frac{3}{2}$, by using the numerical result $e_0 = -2.82833(1)$ [41] based on DMRG estimates for finite systems and the finite-size corrections to the energy, as derived from the Wess-Zumino-Witten theory [42]. The first two terms in the series (35) for $S = \frac{3}{2}$ give the result $e_0 = -2.79507$. In this case, an inclusion of the next-order term in (35) produces the precise SWT result $e_0 = -2.82808$. Thus, already for $S = \frac{3}{2}$ the spin-wave series shows a good convergence.

Turning to the magnon spectrum (36), we find that for $S = \frac{1}{2}$ SWT qualitatively reproduces Des Cloizeaux and Pearson's exact result for the one-magnon triplet excitation spectrum $E_k = \frac{\pi}{2}|\sin k|$ [43]. It is interesting that the $1/S$ correction in (36) improves the standard LSWT result for the spin-wave velocity ($c = 1$) to the value $c = 1.3634$: the exact result is $c = \pi/2 \approx 1.5708$. The magnon spectrum (36) is doubly degenerate and has the relativistic form $E_k = c|k|$ ($c|\pi - k|$) near the point $k = 0$ ($k = \pi$), to be compared with the rigorous result where the spin-wave states, being eigenstates of spin 1, are triply degenerate. Long-wavelength spin waves correspond to states where all regions are locally in a Néel ground state but the direction of the sublattice magnetization makes long-wavelength rotations.

Using (20) and (30), we find the following expression for the on-site magnetization in the antiferromagnetic chain

$$m = S - c_1 = S + \frac{1}{2} - \frac{1}{2N}\sum_k \frac{1}{|\sin k|} = -\infty\,. \tag{37}$$

We see that in $1D$ the quantum correction is divergent at small wave vectors already in the leading LSWT approximation, no matter how large is S. This indicates that the Néel state is destabilized by quantum fluctuations, so that the concept of spin-wave expansion fails.

Finally, it is instructive to calculate the long-wavelength behavior of the correlation function $\langle \boldsymbol{s}_n \cdot \boldsymbol{\sigma}_{n+x}\rangle$. Using the Dyson–Maleev representation and (15), one finds $\langle \boldsymbol{s}_n \cdot \boldsymbol{\sigma}_{n+x}\rangle = -S^2 + 2S\langle a_n b_{n+x}\rangle + \cdots$ where $\langle a_n b_{n+x}\rangle = -(1/2N)\sum_k (\cos k/|sink|)\exp(\mathrm{i}kx)$. Thus, in the limit $x \gg 1$ one obtains

$$\langle \boldsymbol{s}_n \cdot \boldsymbol{\sigma}_{n+x}\rangle = -S^2\left[1 - \frac{1}{\pi S}\ln x + \mathcal{O}\left(\frac{1}{S^2}\right)\right]. \tag{38}$$

This indicates that in the semiclassical limit $S \to \infty$ the antiferromagnetic chain is ordered at exponentially large scales $\xi \simeq a_0 \exp(\pi S)$ [44]. Here we have restored the lattice spacing a_0.

3.2 Spin Wave Interactions

We have already discussed some effects of the quasiparticle interaction V, by calculating the first-order correction to the sublattice magnetizations m_A and m_B. Notice that $\mathcal{O}(\lambda)$ corrections to the ground-state energy (19) as well as to the dispersion functions (22) do not appear. Indeed, it is easy to see that the corresponding matrix elements $\langle 0|V|0\rangle$ and $\langle n_k|V|n_k\rangle$ ($|n_k\rangle = \alpha_k^\dagger|0\rangle$, or $\beta_k^\dagger|0\rangle$) vanish as a result of the normal ordering of V. It will be shown below that the $\mathcal{O}(\lambda^2)$ corrections lead to further improvement of the spin-wave results. To that end, we consider two examples, i.e. the ground-state energy E_0 and the dispersion function $\omega_k^{(\alpha)}$. The reader is referred to the original literature for similar calculations concerning the parameters m_A, ϱ_s [31], and $\Delta_0^{(\beta)}$ [29].

The calculations may be performed within the standard perturbation formula

$$E_i^{(2)} = \sum_{j\neq i} \frac{\langle i|V|j\rangle\langle j|V|i\rangle}{E_i - E_j} \tag{39}$$

giving the second-order correction in V to the eigenvalue E_i of the eigenstate $|i\rangle$ of a non-perturbed Hamiltonian. In our case, the zeroth-order Hamiltonian is $E_0 + \mathcal{H}_D$, and the perturbation V is given by (12). The sum in (39) runs over the eigenstates of $\mathcal{H}_D$.

Second-Order Corrections to E_0

We consider corrections to the vacuum state $|i\rangle \equiv |0\rangle$, so that the energy $E_i \equiv E_0$ is given by (19). There are two types of $\mathcal{O}(\lambda^2)$ corrections to E_0 which are connected with the interactions V_2 and V_{DM}.

First, we proceed with the quadratic interaction V_2. It is easily seen that only the states $|j\rangle \equiv |n_k\rangle = \alpha_k^\dagger\beta_k^\dagger|0\rangle$ produce non-zero matrix elements in (39). The dominator for these two-boson states reads $E_0 - E_k = -2S(\omega_k^{(\alpha)} + \omega_k^{(\beta)})$, where

$\omega_k^{(\alpha,\beta)}$ are defined by (22). Using the above results and (33), we get the following correction to the ground-state energy (19) coming from V_2:

$$E_0^{(2)'} = -\frac{1}{2S}\sum_k \frac{V_k^{(+)}V_k^{(-)}}{\omega_k^{(\alpha)}+\omega_k^{(\beta)}}\,. \tag{40}$$

Next, we consider the Dyson–Maleev interaction V_{DM}. Looking at the explicit expression of V_{DM} (25), we find that only the term with the vertex function $V^{(7)}_{12;34}$ ($V^{(8)}_{12;34}$) does not annihilate the vacuum state $|0\rangle$ ($\langle 0|$). Thus, the sum in (39) runs over the four-boson eigenstates $|1234\rangle = (2!2!)^{-1/2}\alpha^\dagger_{k_1}\alpha^\dagger_{k_2}\beta^\dagger_{k_3}\beta^\dagger_{k_4}|0\rangle$. The related matrix elements read

$$\langle 1234|V_{DM}|0\rangle = -\frac{1}{N}V^{(7)}_{12;34}\delta^{34}_{12}\,, \qquad \langle 0|V_{DM}|1234\rangle = -\frac{1}{N}V^{(8)}_{43;12}\delta^{34}_{12}\,.$$

Using these expressions, we find the following correction to the ground-state energy resulting from V_{DM}:

$$E_0^{(2)''} = -\frac{1}{2S}\frac{1}{N^2}\sum_{1-4}\delta^{34}_{12}\frac{V^{(8)}_{43;12}V^{(7)}_{12;34}}{\omega_1^{(\alpha)}+\omega_2^{(\alpha)}+\omega_3^{(\beta)}+\omega_4^{(\beta)}}\,. \tag{41}$$

Notice that the second-order correction to E_0 in powers of $1/S$ is the sum of $E_0^{(2)'}$ and $E_0^{(2)''}$ but calculated with the bare dispersion functions.

Second-Order Corrections to $\omega_k^{(\alpha)}$

Now we are interested in perturbations to the one-magnon states $|i\rangle \equiv |k\rangle = \alpha_k^\dagger|0\rangle$. The calculations may be performed by following the method already used for E_0. Since we are treating an excited eigenstate, there appear new types of corrections connected to the vertex functions $V^{(2)}_{12;34}$ and $V^{(3)}_{12;34}$. These terms may be predicted, e.g. by drawing the diagrams shown in Fig. 4. Notice that the graphical representation of the vertex functions in Fig. 4 is connected to the quasiparticle operator forms of V_2 (23) and V_{DM} (25). The interested reader is referred to the original literature (see, e.g. [9, 17, 45]) where this diagram technique is explained in detail. We leave these simple calculations as an exercise, and directly present the expression for the second-order corrections to $\omega_k^{(\alpha)}$:

$$\delta\omega_k^{(\alpha)} = -\frac{1}{(2S)^2}\left[\frac{V_k^{(+)}V_k^{(-)}}{\omega_k^{(\alpha)}+\omega_k^{(\beta)}} - \frac{2}{N}\sum_p \frac{V_p^{(+)}V^{(2)}_{kp;pk}+V_p^{(-)}V^{(3)}_{kp;pk}}{\omega_p^{(\alpha)}+\omega_p^{(\beta)}}\right.$$
$$\left. +\frac{2}{N^2}\sum_{2-4}\delta^{34}_{k2}\left(\frac{V^{(8)}_{43;2k}V^{(7)}_{k2;34}}{\omega_k^{(\alpha)}+\omega_2^{(\alpha)}+\omega_3^{(\beta)}+\omega_4^{(\beta)}}+\frac{V^{(3)}_{43;2k}V^{(2)}_{k2;34}}{-\omega_k^{(\alpha)}+\omega_2^{(\beta)}+\omega_3^{(\alpha)}+\omega_4^{(\alpha)}}\right)\right]. \tag{42}$$

It is interesting to note that the vertex functions $V_k^{(-)}$, $V^{(2)}_{kp;pk}$, $V^{(3)}_{kp;pk}$, $V^{(8)}_{43;2k}$, and $V^{(3)}_{43;2k}$ vanish at the zone center $k = 0$ [1], so that the gapless structure of $\omega_k^{(\alpha)}$ is preserved separately by each of the second-order corrections in (42). Thus, we have an example demonstrating some of the good features of the Dyson–Maleev formalism.

[1] Analytical properties of the vertex functions have been studied in [46]

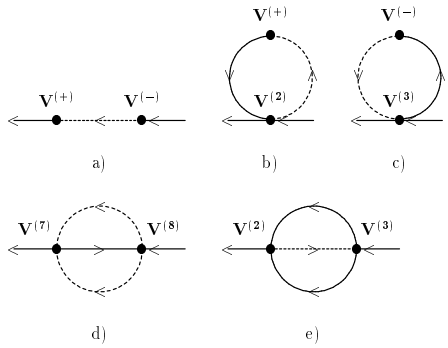

Fig. 4. Second-order self-energy diagrams giving the corrections to the dispersion function $\omega_k^{(\alpha)}$. Solid and dashed lines represent, respectively, the bare propagators for α and β magnons. The Figure is taken from [29].

3.3 Comparison with Numerical Results

We have already presented in Figs. 2 and 3 second-order SWT results for the dispersion functions $\omega_k^{(\alpha,\beta)}$ and the on-site magnetization m_A of the $(1, \frac{1}{2})$ ladder. The comparison shows that the SWT dispersion functions closely follow the ED data in the whole Brillouin zone. For instance, the SWT result for the gap $\Delta_0^{(\beta)}$ at $J_\perp = 0.1$ differs by less than 0.5% from the ED estimate. Turning to m_A, we find a precision higher than 0.3% in the whole interval $0 \leq J_\perp \leq 3$. These are illuminating results, as in the considered system the perturbation parameter $1/S = 2$ is large. To understand these results, let us consider, e.g. the λ series for the spectral gap $\Delta_0^{(\beta)}$ of the $(1, \frac{1}{2})$ chain [29]:

$$\frac{\Delta_0^{(\beta)}}{2(s_1 - s_2)} = 1.6756\lambda^0 + 0.1095\lambda^2 - 0.0107\lambda^3 + \mathcal{O}(\lambda^4)\,.$$

Although $1/S = 2$, we see that the quasiparticle interaction V introduces numerically small corrections to the zeroth-order approximation $\mathcal{H}_D$.

Table 1. Spin-wave results for the parameters $\mathrm{e}_0 = E_0/N$, m_A, and $\Delta_0 = \Delta_0^{(\beta)}/2(s_1 - s_2)$ of different (s_1, s_2) Heisenberg chains calculated, respectively, up to the orders $1/S$, $1/S^2$, and $1/S^3$. The SWT results are compared with available DMRG estimates which are, respectively, denoted by $\bar{\mathrm{e}}_0$, $\bar{m}_A$[39], and $\bar{\Delta}_0$ [47].

(s_1, s_2)	e_0	$\bar{\mathrm{e}}_0$	m_A	$\bar{m}_A$	Δ_0	$\bar{\Delta}_0$
$\left(1, \frac{1}{2}\right)$	-1.45432	-1.45408	0.79388	0.79248	1.7744	1.76
$\left(\frac{3}{2}, 1\right)$	-3.86321	-3.86192	1.14617	1.14427	1.6381	1.63
$\left(\frac{3}{2}, \frac{1}{2}\right)$	-1.96699	-1.96727	1.35666	1.35742	1.4217	1.42
$\left(2, \frac{1}{2}\right)$	-2.47414		1.88984		1.2938	1.29

Finally, in Table 1 we have collected SWT results for different ferrimagnetic chains. It is interesting to note that even in the extreme quantum cases $(1, \frac{1}{2})$ and $(\frac{3}{2}, 1)$, deviations from the DMRG estimates are less than 0.03% for the energy and 0.2% for the on-site magnetization. Moreover, it is seen that the increase of $r_s = s_1/s_2$ – keeping $s_2 = \frac{1}{2}$ fixed – leads to a rapid improvement of the $1/S$ series. The above results suggest that the Heisenberg ferrimagnetic chains and ladders are examples of low-dimensional quantum spin systems where the spin-wave approach is an effective theoretical tool.

4 Applications to 2D Heisenberg Antiferromagnets

In this Sect. we survey recent applications of the spin-wave approach to 2D Heisenberg spin systems, the emphasis being on the ground-state parameters of the square- and triangular-lattice Heisenberg antiferromagnets. We shall skip most of the technical details, as the discussed spin-wave formalism actually does not depend on the space dimension. As already mentioned, for the last decade SWT has been found to produce surprisingly accurate results for the ground-state parameters of the square-lattice Heisenberg antiferromagnet even in the extreme quantum limit $S = \frac{1}{2}$. Below we collect these results and compare them with recent QMC numerical estimates. As to the triangular antiferromagnet, it seems to be a rare example of magnetically frustrated spin system where the spin-wave expansion is effective. In this case, we also give some technical details concerning the spin-wave expansion, as it includes some new issues resulting from the coplanar arrangement of classical spins.

4.1 Square-Lattice Antiferromagnet

The square-lattice $S = \frac{1}{2}$ Heisenberg antiferromagnet – being a simple and rather general model to describe the undoped copper-oxide materials – has received a great deal of interest for the last decade. Now it is widely accepted that the ground state of the model is characterized by antiferromagnetic long-rage order. Thus, the role of quantum spin fluctuations is restricted to reduction of the sublattice magnetization from its classical value $\frac{1}{2}$ by about 39%. [2] In a seminal work by Chakravarty, Halperin, and Nelson [48] – using the renormalization-group approach to study the quantum non-linear σ model in $2+1$ space-time dimension – it has been shown that in the so-called renormalized classical regime $k_B T \ll \rho_s$ the thermodynamic properties of the 2D quantum Heisenberg antiferromagnet are dominated by magnon excitations, so that the leading and next-to-leading corrections in $k_B T/\rho_s$ are fully controlled by three physical parameters, i.e the spin stiffness constant ρ_s,[3] the spin-wave velocity c, and the on-site magnetization m, calculated at $T = 0$ (see also [49]).

[2] Compare with the reduction of about 42% of the classical on-site magnetization $\frac{1}{2}$ in the $(1, \frac{1}{2})$ ferrimagnetic chain (see Table 1).

[3] This quantity, measuring the response of the system to an infinitesimal twist of the spins around an axis perpendicular to the direction of the broken symmetry, should not be confused with the spin stiffness constant of the ferromagnetic state ϱ_s connected to the Landau–Lifshitz relation (26).

Moreover, it has been argued that the discussed universal thermodynamic properties appear for arbitrary k_BT/ρ_s, provided that $0 < \rho_s \ll J$ and $k_BT \ll J$, J being the nearest-neighbor exchange constant [50].

The quantities ρ_s, and c appear as input parameters in the quantum non-linear σ model defined by the Lagrangian density

$$\mathcal{L} = \frac{\rho_s}{2c^2}\left(\frac{\partial \boldsymbol{n}}{\partial t}\right)^2 - \frac{\rho_s}{2}\left[\left(\frac{\partial \boldsymbol{n}}{\partial x}\right)^2 + \left(\frac{\partial \boldsymbol{n}}{\partial y}\right)^2\right], \tag{43}$$

where the vector staggered field $\boldsymbol{n} = \boldsymbol{n}(t, x, y)$ satisfies the non-linear constraint $\boldsymbol{n}^2 = 1$. This model may be introduced using arguments based on general grounds: As long as the continuous $O(3)$ symmetry is spontaneously broken, the symmetry of the problem requires that the interaction of the Goldstone modes, i.e. spin waves, of the system in the long-wavelength limit be described by this model regardless of the details of the macroscopic Hamiltonian and the value of the spin. For the square-lattice antiferromagnet, close to $\boldsymbol{k} = (0, 0)$ and (π, π) the magnon spectrum takes the relativistic forms $E_{\boldsymbol{k}} = c|\boldsymbol{k}|$ and $|\boldsymbol{\pi} - \boldsymbol{k}|$, c being the spin-wave velocity. If we expand $\boldsymbol{n}$ as $(1, \epsilon_1, \epsilon_2)$, where the ϵ_i are small compared to unity, then the equations of motion following from (43) show that there are two modes both of which have the dispersion $E_{\boldsymbol{k}} = c|k|$, as expected. If we expand the Lagrangian to higher orders in ϵ_i, we find that there are interactions between the spin waves whose strength is proportional to c/ρ_s, which is of order $1/S$. We thus see that all the parameters appearing in (43) can be determined by SWT. Compared to the standard $1/S$ expansion, the hydrodynamic approach is more generic in two points, i.e. (i) it is applicable to magnetically disordered phases, and (ii) it may lead to non-perturbative results which are beyond the reach of SWT (see, e.g. [51, 52, 53]).

Ground-state parameters of the $S = \frac{1}{2}$ square-lattice Heisenberg antiferromagnet have been studied in great detail using a variety of techniques, including SWT, QMC, and series expansions [15]. An early QMC study by Reger and Young [54] indicated that the SWT gives a good quantitative description of the ground state. Series expansions around the Ising limit performed by Singh [55, 56] found the results $\rho_s \approx 0.18J$ and $c \approx 1.7J$, both in good agreement with the first-order SWT [6]. Later on, higher-order calculations demonstrated that the second-order corrections in $1/S$ to the parameters ρ_s, c and m are small – even in the extreme quantum limit $S = \frac{1}{2}$ – and improve the SWT results. For instance – using both the Dyson–Maleev and Holstein–Primakoff formalisms up to second order in $1/S$ – Hamer et al. calculated the ground-state energy E_0/N and the sublattice magnetization m [36]. Both formalisms were shown to give identical results closely approximating previous series estimates [57]. Different scientific groups have presented consistent second-order SWT results for the spin-wave velocity c [58, 59, 60], the uniform transverse susceptibility $\chi_\perp$[59, 61] and the spin stiffness constant ρ_s[4] [59, 61]. In Table 2 we have collected some of these results, demonstrating an excellent agreement with recent high-precision numerical estimates [37] obtained by using the stochastic series expansion QMC method for $L \times L$ lattices with L up to 16.

The accuracy of SWT may be understood in terms of the spin-wave interaction V. Indeed, let us consider the $1/S$ series for m [36]

[4] The reported third-order SWT result for this parameter is 0.1750(1)[61].

Table 2. Second-order SWT results for the ground-state energy per site $e_0 = E_0/N$ [36], the on-site magnetization m [36, 59], the spin-wave velocity c [59, 60], the uniform transverse susceptibility $\chi_\perp$ [59, 61], and the spin stiffness constant ρ_s [59, 61] of the $S = \frac{1}{2}$ square-lattice Heisenberg antiferromagnet. The SWT results are compared to recent stochastic series expansion QMC estimates for $L \times L$ lattices with L up to 16 [37]. The series risults for e_0, m and $\chi_\perp$ are taken from [62], and those for ρ_s and c – from [61]. The figures in parentheses show the errors in the last significant figure. $\hbar = a_0 = J = 1$.

Quantity	SWT	QMC	Series
$-e_0$	0.669494(4)	0.669437(5)	0.6693(1)
m	0.3069(1)	0.3070(3)	0.307(1)
c	1.66802(3)	1.673(7)	1.655(12)
$\chi_\perp$	0.06291(1)	0.0625(9)	0.0659(10)
ρ_s	0.180978	0.175(2)	0.182(5)

$$m = S - 0.1966019 + \frac{0.003464}{(2S)^2} + \mathcal{O}\left(\frac{1}{S^3}\right) . \tag{44}$$

For $S = \frac{1}{2}$, the related series in powers of λ simply reads $m = 0.3033981\lambda^0 + 0.003464\lambda^2 + \mathcal{O}(\lambda^3)$, so that the spin-wave interaction V introduces numerically small corrections to the leading approximation. The same conclusion is valid for the other parameters.

4.2 Triangular-Lattice Antiferromagnet

The Heisenberg antiferromagnet on a triangular lattice with nearest-neighbor exchange interactions is a typical example of strongly frustrated spin model.[5]

After a long period of intensive studies – see, e.g. [64] and references therein – it is now widely accepted that the classical coplanar ground state survives quantum fluctuations. This state may be represented by the ansatz

$$\frac{\boldsymbol{s_r}}{S} = \hat{\boldsymbol{z}} \cos(\boldsymbol{q}_M \cdot \boldsymbol{r}) + \hat{\boldsymbol{x}} \sin(\boldsymbol{q}_M \cdot \boldsymbol{r}) , \tag{45}$$

where $\boldsymbol{q}_M = (\frac{4\pi}{3}, 0)$ is the wave vector of the magnetic pattern, $\hat{\boldsymbol{x}} \perp \hat{\boldsymbol{z}}$ are unit coordinate vectors in the spin space, and $\boldsymbol{r}$ runs on the lattice sites. As usual, the lattice spacing a_0 is set to unity. The classical spins lay in the (x, z) plane, and point in three different directions so that the angle $\frac{2\pi}{3}$ is settled between any pair of spins in the elementary triangle $(\boldsymbol{s}_a, \boldsymbol{s}_b, \boldsymbol{s}_c)$.

In performing the $1/S$ expansion about non-collinear reference states such as (45), one faces some novelties which will be discussed in the remainder of this Sect. One of them concerns the number of boson fields needed to keep track of the whole magnon spectrum. This is an important practical issue, as higher-order spin-wave expansions involving more than two boson fields are, as a rule, technically intractable. In the general case, this number should be equal to the number

[5] For a recent review on frustrated quantum magnets, see [63].

of spins in the magnetic elementary cell, so that for the magnetic structure (45) we would need three boson fields. However, in several special cases we can transform the non-collinear magnetic structures into a ferromagnetic configuration by applying a uniform twist on the coordinate frame. These special systems have the property that their magnon spectrum has no gaps at the boundaries of the reduced magnetic Brillouin zone connected to the magnetic pattern. The triangular-lattice antiferromagnet fulfills this rule, so that we may describe the system by a single boson field, as in the ferromagnetic case. In the remainder of this Sect. we shall follow this approach [65].

To that end, let us rotate the spin coordinate frame about the y axis by the angle $\theta_{\boldsymbol{r}\boldsymbol{r}'} = \boldsymbol{q}_M \cdot (\boldsymbol{r} - \boldsymbol{r}')$ for any pair of neighboring spins $(\boldsymbol{s}_{\boldsymbol{r}}, \boldsymbol{s}_{\boldsymbol{r}'})$, in accord to the reference state (45). In the local reference frame, the Heisenberg Hamiltonian acquires the form

$$\mathcal{H} = \sum_{(\boldsymbol{r},\boldsymbol{r}')} \left[\cos\theta_{\boldsymbol{r}\boldsymbol{r}'} \left(s^x_{\boldsymbol{r}} s^x_{\boldsymbol{r}'} + s^z_{\boldsymbol{r}} s^z_{\boldsymbol{r}'} \right) + \sin\theta_{\boldsymbol{r}\boldsymbol{r}'} \left(s^z_{\boldsymbol{r}} s^x_{\boldsymbol{r}'} - s^x_{\boldsymbol{r}} s^z_{\boldsymbol{r}'} \right) + s^y_{\boldsymbol{r}} s^y_{\boldsymbol{r}'} \right], \tag{46}$$

where the sum runs over all pairs of nearest-neighbor sites of the triangular lattice.

Next, using the Holstein–Primakoff transformation (4)[6] and the procedures described in Sect. 2, we find the following boson representation for (46)

$$\mathcal{H}_B = -\frac{3}{2} S^2 N + 3S \sum_{k} \left[A_{\boldsymbol{k}} a^\dagger_{\boldsymbol{k}} a_{\boldsymbol{k}} + \frac{B_{\boldsymbol{k}}}{2} \left(a^\dagger_{\boldsymbol{k}} a^\dagger_{-\boldsymbol{k}} + a_{\boldsymbol{k}} a_{-\boldsymbol{k}} \right) \right] + V\,, \tag{47}$$

$A_{\boldsymbol{k}} = 1 + \nu_{\boldsymbol{k}}/2$, $B_{\boldsymbol{k}} = -3\nu_{\boldsymbol{k}}/2$, and $\nu_{\boldsymbol{k}} = \frac{1}{3}[\cos k_x + 2\cos(k_x/2)\cos(\sqrt{3}k_y/2)]$. Here and in the remainder of this Sect., $\boldsymbol{k}$ takes N values from the first Brillouin zone of the triangular lattice.

Up to quartic anharmonic terms, the expansion of the square root in (46) produces the following spin-wave interaction $V = V_3 + V_4$, where

$$V_3 = \mathrm{i}\sqrt{\frac{S}{2}} \frac{3}{2\sqrt{N}} \sum_{1-3} (\kappa_1 + \kappa_2)(a^\dagger_1 a^\dagger_2 a_3 - a^\dagger_3 a_2 a_1)\,, \tag{48}$$

$$V_4 = -\frac{3}{16N} \sum_{1-4} \left[\Gamma^{(1)}_{12;34} a^\dagger_1 a^\dagger_2 a_3 a_4 + \Gamma^{(2)}_{123} (a^\dagger_1 a^\dagger_2 a^\dagger_3 a_4 + a^\dagger_4 a_3 a_2 a_1) \right], \tag{49}$$

$\kappa_{\boldsymbol{k}} = \frac{1}{3}[\sin k_x - 2\sin(k_x/2)\cos(\sqrt{3}k_y/2)]$, $\Gamma^{(1)}_{12;34} = 4\nu_{1-3} + 4\nu_{2-3} + \nu_1 + \nu_2 + \nu_3 + \nu_4$, and $\Gamma^{(2)}_{123} = -2(\nu_1 + \nu_2 + \nu_3)$. For simplicity, in the last expressions we have omitted the Kronecker δ function, and have used the abbreviations for the wave vectors introduced in Sect. 2.2.

A novelty here is the triple boson interaction $V_3 = \mathcal{O}(S^{1/2})$, which is typical for systems exhibiting non-collinear magnetic patterns. We shall see below that such kind of interactions complicate the calculation of higher-order $1/S$ corrections.

[6] The choice of the transformation is a matter of convenience, as the final results – at least to second order in $1/S$ – are independent of the boson representation.

Linear Spin Wave Approximation

In a standard LSWT, we discard V and diagonalize the quadratic part of (47) by the Bogoliubov transformation $a_{\boldsymbol{k}} = u_{\boldsymbol{k}}(\alpha_{\boldsymbol{k}} - x_{\boldsymbol{k}}\alpha^{\dagger}_{-\boldsymbol{k}})$. The parameters $u_{\boldsymbol{k}}$ and $x_{\boldsymbol{k}}$ are defined by (16) and (17), but in this case $\eta_{\boldsymbol{k}} = -3\nu_{\boldsymbol{k}}/(2+\nu_{\boldsymbol{k}})$. The diagonalization yields the free-quasiparticle Hamiltonian $\mathcal{H}_0 = 3S\sum_{\boldsymbol{k}} \omega_{\boldsymbol{k}} \alpha^{\dagger}_{\boldsymbol{k}} \alpha_{\boldsymbol{k}}$, where the dispersion function

$$E_{\boldsymbol{k}} \equiv 3S\omega_{\boldsymbol{k}} = 3S\sqrt{(1-\nu_{\boldsymbol{k}})(1+2\nu_{\boldsymbol{k}})} \tag{50}$$

gives the magnon energies in a LSWT approximation, to be compared with the magnon spectrum resulting from the approach using three boson fields [66]. It is easy to check that the dispersion function (50) exhibits three zero modes, as it should be since the Hamiltonian symmetry $O(3)$ is completely broken by the magnetic pattern (45). Two of these modes are at the ordering wave vectors $\boldsymbol{k} = \pm\boldsymbol{q}_M$, whereas the third zero mode at $\boldsymbol{k} = 0$ describes soft fluctuations of the total magnetization. Expanding about the zero modes, we find the following expressions for the spin-wave velocities [67]

$$c_{0\perp} \equiv c_{\pm q_M} = \left(\frac{3}{2}\right)^{3/2} S\,, \qquad c_{0\parallel} \equiv c_{k=0} = \frac{3\sqrt{3}}{2} S\,. \tag{51}$$

Let us now calculate the on-site magnetization $m = \langle s^z_{\boldsymbol{r}}\rangle = S - \langle a^{\dagger}_{\boldsymbol{r}} a_{\boldsymbol{r}}\rangle$. Using the Bogoliubov transformation, we find for the density of particles $\langle a^{\dagger}_{\boldsymbol{k}} a_{\boldsymbol{k}}\rangle = -1/2 + 1/(2\varepsilon_{\boldsymbol{k}})$, so that the LSWT result for m reads [66]

$$m = S + \frac{1}{2} - \frac{1}{2N}\sum_{\boldsymbol{k}} \frac{1}{\sqrt{1-\eta^2_{\boldsymbol{k}}}} = S - 0.2613\,. \tag{52}$$

For $S = \frac{1}{2}$, the LSWT result is $m = 0.2387$. Since the reported leading $1/S$ correction to m is small and positive[7], there is a clear disagreement with the recent QMC estimate $m = 0.20(6)$ [69].

Spin Wave Interactions

Here we consider as an example the calculation of $1/S$ corrections to the magnon spectrum (50). There are two different types of corrections related to the spin-wave interactions V_3 and V_4 in (48). Turning to V_4, notice that we have already learned (Sect. 2.3) that the required correction may be obtained by expressing V_4 as a sum of normal products of quasiparticle operators: the diagonal quadratic terms give the required $1/S$ correction to the spectrum. However, in several cases we are not interested in the quasiparticle representation of V_4. Then, it is possible to follow another way by decoupling the quartic operator products in V_4. Actually, this procedure takes into account the so-called one-loop diagrams, and may be performed within a formal substitution of the operator products, such as $a^{\dagger}_1 a^{\dagger}_2 a_3 a_4$, by the following sum over all the non-zero pair boson correlators

[7] We are aware of two such calculations reporting, however, somewhat different corrections, i.e. $0.0055/S$ [68] and $0.00135/S$ [65].

$$a_1^\dagger a_2^\dagger a_3 a_4 \longmapsto \sum_{\text{pair}} \left[\langle a_1^\dagger a_2^\dagger \rangle a_3 a_4 + a_1^\dagger a_2^\dagger \langle a_3 a_4 \rangle - \langle a_1^\dagger a_2^\dagger \rangle \langle a_3 a_4 \rangle \right] . \tag{53}$$

As suggested by the quadratic form in (47), there are two types of boson correlators, i.e. $\langle a_1^\dagger a_2 \rangle$ and $\langle a_1 a_2 \rangle = \langle a_1^\dagger a_2^\dagger \rangle$, contributing in (53). The constant terms in (53) give first-order corrections to the ground state energy, whereas the quadratic operator products renormalize the coefficients $A_{\boldsymbol{k}}$ and $B_{\boldsymbol{k}}$ in (47). Thus, the interaction V_4 renormalizes the bare dispersion function $\omega_{\boldsymbol{k}}$ to

$$\bar{\omega}_{\boldsymbol{k}} = \sqrt{\bar{A}_{\boldsymbol{k}}^2 - \bar{B}_{\boldsymbol{k}}^2} , \tag{54}$$

where the new coefficients $\bar{A}_{\boldsymbol{k}}$ and $\bar{B}_{\boldsymbol{k}}$ can be expressed in the form[8]

$$\bar{A}_{\boldsymbol{k}} = A_{\boldsymbol{k}} \left(1 + \frac{a_1}{2S} \right) + \frac{a_2}{2S} , \qquad \bar{B}_{\boldsymbol{k}} = B_{\boldsymbol{k}} \left(1 + \frac{b_1}{2S} \right) + \frac{b_2}{2S} .$$

An analysis of (54) indicates that the renormalized spectrum still preserves the zero mode at $\boldsymbol{k} = 0$, but at the same time acquires non-physical gaps at $\boldsymbol{k} = \pm \boldsymbol{q}_M$. The reason for such kind of behavior of the SWT is connected with the fact that we have omitted the $1/S$ corrections resulting from V_3. Indeed, the spin-wave interaction V_3 has the order $\mathcal{O}(S^{1/2})$, so that a simple power counting indicates that $1/S$ corrections to $\omega_{\boldsymbol{k}}$ appear in the second-order of the perturbation theory in V_3. We shall skip the details of this calculation, as it may be performed entirely in the framework of the method presented in Sect. 2. Namely, one should express V_3 in terms of quasiparticle operators, and then apply the general perturbation formula (32) for the interaction V_3, by using the dressed dispersions (54). As a matter of fact, as we are interested in corrections up to $1/S$, we can use the bare dispersion function (50). The final result of this calculation shows that the $1/S$ correction resulting from V_3 exactly vanishes the gap (produced by V_4), so that the structure of magnon spectrum (50) – containing three zero modes – is preserved in the leading first-order approximation [70]. Based on the renormalized dispersion, the following expressions for the spin-wave velocities (51) have been reported [65]:

$$c_\parallel = c_{0\parallel} \left(1 - \frac{0.115}{2S} \right) , \qquad c_\perp = c_{0\perp} \left(1 + \frac{0.083}{2S} \right) .$$

Notice that the $1/S$ corrections diminish the ratio $c_\parallel / c_\perp$ from the LSWT result 1.41 to the value 1.16. These expressions indicate that the leading corrections to the magnon spectrum are numerically small even in the case $S = \frac{1}{2}$. Good convergence has been found also for the $1/S$ series of the magnetic susceptibilities $\chi_\perp$ and $\chi_\parallel$ [71, 72] which appear as parameters of the magnetic susceptibility tensor [73]

$$\chi_{\alpha\beta} = \chi_\perp \delta_{\alpha\beta} + (\chi_\parallel - \chi_\perp) y_\alpha) y_\beta .$$

Here $\hat{\boldsymbol{y}}$ is a unit vector directed perpendicular to the basal (x, z) plane of the planar magnetic structure.

Summarizing, the available SWT results point towards a good convergence of the perturbative spin-wave series in the triangular-lattice Heisenberg antiferromagnet. This is remarkable, as the spin-wave expansion might have been expected to fail for strongly frustrated magnetic systems.

[8] For brevity, here we omit the expressions for the constants a_1, a_2, b_1, and b_2 [65].

5 Modified Spin Wave Theories

Here we consider some modifications of the standard spin-wave theory allowing for an analysis of magnetically disordered phases. These may appear either as a result of quantum fluctuations – a classical example being the spin-S Heisenberg antiferromagnetic chain discussed in Sect. 3.1 – or due to thermal fluctuations, as in $1D$ and $2D$ Heisenberg magnets with short-range isotropic interactions [14]. For the antiferromagnetic chain, we have indicated that the failure of SWT arises already in the linear spin-wave approximation as a divergency in the boson-occupation numbers $n_i = \langle a_i^\dagger a_i \rangle = \infty$ implying $\langle s_i^z \rangle = -\infty$. Infinite number of spin waves also appears at $T > 0$, when the $T = 0$ magnetic phases of low-dimensional Heisenberg systems do not survive thermal fluctuations. Actually, the occupation numbers n_i should not exceed $2S$ – as dictated by the spin algebra – and the magnetization should be zero, as required by the symmetry of the phases. In the remainder of this Sect. we discuss modifications of the SWT based on *ad hoc* constraints imposing fixed number of bosons.

The first generalized spin-wave theory of this kind has been formulated by Takahashi to study the low-T thermodynamics of $1D$ and $2D$ Heisenberg ferromagnets [74, 75]. Takahashi's idea was to supplement the standard SWT of Heisenberg ferromagnets with the constraint imposing zero ferromagnetic moment at $T > 0$:

$$M = \sum_{n=1}^{N} \langle s_n^z \rangle = SN - \sum_{\boldsymbol{k}} \langle a_{\boldsymbol{k}}^\dagger a_{\boldsymbol{k}} \rangle = 0 \,. \tag{55}$$

Depending on the context, in the remainder of this Sect. $\langle A \rangle$ means the expectation value of the operator A at $T = 0$ or $T > 0$. Quite surprisingly, it was found an excellent agreement with the Bethe-ansatz low-temperature expansions of the free energy and magnetic susceptibility for the $S = \frac{1}{2}$ Heisenberg ferromagnetic chain. Similar extensions of SWT have been suggested for Heisenberg antiferromagnets both at $T = 0$ [76, 77] and at $T > 0$ [78, 79], by using the same constraint equation (55) but for the sublattice magnetization. Below we discuss some applications of the modified SWT to low-dimensional Heisenberg antiferromagnets both at $T = 0$ and at finite temperatures.

5.1 Square-Lattice Antiferromagnet at Finite T

Using the Dyson–Maleev transformations (9) and (10), the boson Hamiltonian $\mathcal{H}_B^{'}$ of the square-lattice antiferromagnet reads

$$\mathcal{H}_B^{'} = -\frac{N}{2} JzS^2 + \sum_{\boldsymbol{k}} \left[A_{\boldsymbol{k}} (a_{\boldsymbol{k}}^\dagger a_{\boldsymbol{k}} + b_{\boldsymbol{k}}^\dagger b_{\boldsymbol{k}}) + B_{\boldsymbol{k}} (a_{\boldsymbol{k}}^\dagger b_{\boldsymbol{k}}^\dagger + a_{\boldsymbol{k}} b_{\boldsymbol{k}}) \right] + V_{DM}^{'} \,, \tag{56}$$

whereas the constraint equation for the total sublattice magnetization takes the form

$$\sum_{\boldsymbol{k}} \langle a_{\boldsymbol{k}}^\dagger a_{\boldsymbol{k}} + b_{\boldsymbol{k}}^\dagger b_{\boldsymbol{k}} \rangle = SN \,. \tag{57}$$

The wave vector $\boldsymbol{k}$ runs in the small (magnetic) Brillouin zone $|k_x \pm k_y| \leq \pi$ containing $N/2$ points. $A_{\boldsymbol{k}} = JSz$, $B_{\boldsymbol{k}} = JSz\gamma_{\boldsymbol{k}}$, $\gamma_{\boldsymbol{k}} = \frac{1}{2}(\cos k_x + \cos k_y)$, and $z = 4$ is the lattice coordination number.

In essence, the constraint equation (57) introduces an effective cut-off for unphysical states [80]. To see this, let us consider the $S = \frac{1}{2}$ system. According to (57), the average number of, say, the α magnons is $N/4$, whereas the total number of one-magnon states in the magnetic Brillouin zone is $N/2$. Thus, after introducing the constraint (57), the effective number of allowed states in the boson Hilbert space is

$$\left[\frac{(N/2)!}{(N/4)!(N/4)!}\right]^2 \sim \frac{4}{\pi}\frac{2^N}{N}\,,$$

so that with logarithmic accuracy the correct dimension 2^N is restored.

To implement the constraint equation in the theory, we introduce, as usual, a chemical potential μ for the boson fields, i.e. instead of $\mathcal{H}_B^{'}$ we consider the Hamiltonian

$$\mathcal{H}_B = \mathcal{H}_B^{'} - \mu \sum_{\boldsymbol{k}} (a_{\boldsymbol{k}}^{\dagger} a_{\boldsymbol{k}} + b_{\boldsymbol{k}}^{\dagger} b_{\boldsymbol{k}})\,, \tag{58}$$

where μ is fixed by the constraint equation (57). Notice that the introduction of a chemical potential simply renormalizes the coefficient $A_{\boldsymbol{k}} \to A_{\boldsymbol{k}} - \mu$ so that we can apply the formalism from Sect. 2 without any changes.

Using the Bogoliubov transformation (15) with the parameter $\eta_{\boldsymbol{k}} = JzS\gamma_{\boldsymbol{k}}/(JzS - \mu)$, one finds the following quasiparticle representation of $\mathcal{H}_B$ (see, e.g. [17])

$$\mathcal{H}_B = E_0 + \mathcal{H}_D + V_{DM}\,, \tag{59}$$

where E_0 is the ground-state energy calculated up to first-order of the perturbation theory in $1/S$:

$$E_0 = -\frac{N}{2} zJS^2 \left(1 + \frac{r}{2S}\right)^2\,, \qquad r = 1 - \frac{2}{N}\sum_{\boldsymbol{k}} \sqrt{1 - \eta_{\boldsymbol{k}}^2}\,. \tag{60}$$

As we know from Sect. 2.3, the free-quasiparticle Hamiltonian

$$\mathcal{H}_D = \sum_{\boldsymbol{k}} E_{\boldsymbol{k}} (\alpha_{\boldsymbol{k}}^{\dagger}\alpha_{\boldsymbol{k}} + \beta_{\boldsymbol{k}}^{\dagger}\beta_{\boldsymbol{k}}) \tag{61}$$

includes the diagonal quadratic terms resulting from $V_{DM}^{'}$, so that the magnon energies $E_{\boldsymbol{k}}$ are calculated up to first-order corrections in $1/S$:

$$E_{\boldsymbol{k}} = JzS \left(1 + \frac{r}{2S}\right) \sqrt{1 - \eta_{\boldsymbol{k}}^2}\,. \tag{62}$$

Here the factor $r/2S$ is Oguchi's correction to the magnon spectrum [6].

We want to treat the spin-wave interaction up to first order in the $1/S$ perturbation theory, so that the Dyson–Maleev interaction V_{DM} will be discarder. It is important to notice that here the off-diagonal quadratic interaction V_2 does not appear, as dictated by the sublattice interchange symmetry. This means that the lowest-order corrections to the sublattice magnetization m have the order $\mathcal{O}(S^{-2})$, see the series (44), so that the constraint equation (57) calculated in a LSWT approximation can be safety used at this level.

Turning to the magnon spectrum (62), we see that the chemical potential introduces a spectral gap Δ so that close to the zone center the excitation spectrum acquires the relativistic form

$$E_{\boldsymbol{k}} = \sqrt{\Delta^2 + c^2 k^2}\,, \qquad c = \frac{JzS}{\sqrt{2}}\left(1 + \frac{r}{2S}\right), \tag{63}$$

where $\Delta = 2c(-\mu/JzS)^{1/2}$ and c is the spin-wave velocity calculated up to first order in $1/S$. Using the standard expression for free bosons $n_{\boldsymbol{k}} = \langle \alpha^\dagger_{\boldsymbol{k}} \alpha_{\boldsymbol{k}} \rangle = \langle \beta^\dagger_{\boldsymbol{k}} \beta_{\boldsymbol{k}} \rangle = [\exp(-E_{\boldsymbol{k}}/k_B T) - 1]^{-1}$, the constraint equation (57) takes the form

$$S + \frac{1}{2} = \frac{1}{N} \sum_{\boldsymbol{k}} \frac{1}{\sqrt{1 - \eta^2_{\boldsymbol{k}}}} \coth \frac{E_{\boldsymbol{k}}}{k_B T}\,. \tag{64}$$

At low T, the main contributions in the last sum come from small wave vectors so that, using (63), the gap equation (64) yields

$$\Delta = \frac{c}{\xi} = 2T \operatorname{arcsinh}\left[\frac{1}{2}\exp\left(-\frac{2\pi\rho_s}{k_B T}\right)\right]. \tag{65}$$

Here ρ_s is the $T = 0$ spin stiffness constant calculated up to first order in $1/S$, and ξ is the spin correlation length. This result exactly reproduces the saddle-point equation in the $1/N$ expansion of the $O(N)$ nonlinear σ model in $2 + 1$ space-time dimensions (see, e.g. [81]). It is well known that (65) describes three different regimes, i.e. (i) the renormalized classical, (ii) the quantum critical, and (iii) the quantum disordered regimes [53].

As an example, we consider the renormalized classical regime defined by the condition $k_B T \ll \rho_s$. In this case, the last equation yields the following result for the correlation length

$$\xi \sim \frac{c}{T}\exp\left(\frac{2\pi\rho_s}{k_B T}\right). \tag{66}$$

This coincides with the one-loop approximation of the $2 + 1$ nonlinear σ model [48]. As is well known, at a two-loop level the T dependence in the pre-exponential factor disappears, whereas the exponent argument does not change.

Finally, let us calculate the leading temperature correction to the internal energy $U = \langle \mathcal{H}_B \rangle$. The expression for U reads

$$U = E_0 + \sum_{\boldsymbol{k}} E_{\boldsymbol{k}} \left(\coth \frac{E_{\boldsymbol{k}}}{k_B T} - 1\right). \tag{67}$$

Using (63), after some algebra one finds the following result:

$$U = E_0 + \frac{2\zeta(3)N}{\pi c^2} T^3\,. \tag{68}$$

Here $\zeta(x)$ is the Riemann zeta function. The above temperature correction describes the contribution from two zero modes, i.e. $\boldsymbol{k} = (0, 0)$ and $\boldsymbol{k} = (\pi, \pi)$, and reproduces the expected universal behavior known from the $2 + 1$ nonlinear σ model and the chiral perturbation theory [49, 82].

5.2 Applications to Finite-Size Systems

The modified SWT can also be applied to finite-size systems [76, 77]. This opens an opportunity directly to compare SWT results with finite-size numerical data.

As is known, the standard SWT is not applicable to finite systems due to divergences related to the Goldstone zero modes. Actually, the divergency comes from the Bogoliubov transformation (15) which is not defined for these modes.

Turning to the example from Sect. 5.1, notice that in the infinite system the chemical potential μ goes to zero as $T \to 0$. At $T = 0$ the constraint equation takes the form

$$S + \frac{1}{2} - \frac{2}{N\sqrt{1-\eta_0^2}} - \frac{1}{N}\sum_{\boldsymbol{k}\neq 0}\frac{1}{\sqrt{1-\eta_{\boldsymbol{k}}^2}} = 0\,. \tag{69}$$

Here we have selected the contribution from the two zero modes at $\boldsymbol{k} = (0,0)$ having $S^z = \pm 1$.

According to (69), on a finite lattice the parameter $\eta_0 = JzS/(JzS - \mu)$ is less than unity, so that the divergences associated with the zero modes disappear. The constraint (69) takes into account the fact that in finite systems there are no spontaneously broken continuous symmetries.

To find the staggered magnetization m appearing in the thermodynamic limit of the $2D$ system, we calculate the antiferromagnetic structure factor $S(\pi,\pi)$ for large N:

$$m^2(N) = \frac{2}{N}S(\pi,\pi) = \frac{4}{(1-\eta_0^2)N^2} + \frac{1}{N^2}\sum_{\boldsymbol{k}\neq 0}\frac{1+\eta_{\boldsymbol{k}}^2}{1-\eta_{\boldsymbol{k}}^2}\,, \tag{70}$$

where we have again selected the contribution from the zero modes.

In the large-N limit, the last sum transforms into an integral which is $\propto \ln N$, so that the main contribution comes from the first term in (70). Thus, we find the relation

$$m^2 = \lim_{N\to\infty}\frac{4}{(1-\eta_0^2)N^2}\,. \tag{71}$$

Equation (69) induces a gap in the magnon spectrum which is defined by $\Delta = c\sqrt{2(1-\eta_0^2)}$. Using (71) and the notations from Sect. 5.1, we find the following result for the magnon excitation gap in the large-N limit

$$\Delta = \frac{c^2}{\rho_s L^2}\,. \tag{72}$$

$L = N^{1/2}$ is the linear size in a square geometry. The last expression reproduces the result for Δ obtained by other methods [83, 84, 49].

Finally, let us return to the Heisenberg antiferromagnetic chain discussed in Sec. 3.1, this time using the modified SWT [79]. We have seen that in $1D$ the expression for the staggered magnetization (37) contained an infrared divergency indicating that the magnetic order is destabilized by quantum fluctuations. Using the concept of the modified theory, we can resolve the problem by replacing (37) with the constraint equation

$$S + \frac{1}{2} = \frac{1}{N}\sum_{k}\frac{1}{\sqrt{1-\eta_0^2\cos^2 k}} = \frac{K(\eta_0)}{\pi}\,, \tag{73}$$

where $K(\eta_0)$ is the complete elliptic integral of the first kind.

Since $K(\eta_0) \geq \pi/2$, the gap equation (73) has a solution for arbitrary S. However, the constraint introduces an excitation gap, so that the discussed theory makes sense only for integer S. To find the gap, we may use for small $(1-\eta_0^2)^{1/2}$ the asymptotic result $K(\eta_0) = \ln 4(1-\eta_0^2)^{-1/2}$, so that the excitation gap reads

$$\Delta \sim c \exp(-\pi S). \tag{74}$$

Here c is the spin-wave velocity of the antiferromagnetic chain (36). The obtained gap has the asymptotic form $\Delta \sim S \exp(-\pi S)$, to be compared with Haldane's result $\Delta \sim S^2 \exp(-\pi S)$ obtained from the σ-model mapping [85, 86]. It is remarkable that the simple modified SWT is capble to reproduce the asymptotic expression for the Haldane gap.

6 Concluding Remarks

We have surveyed the spin-wave technique and its typical applications to Heisenberg magnetic systems in restricted geometries. In most of the cases the SWT results were compared with the available numerical estimates. As a result, the systematic large-S technique has been found to give very accurate description of the zero-temperature parameters and magnon excitation spectra of a number of low-dimensional quantum spin models, such as the Heisenberg antiferromagnet on square and triangular lattices and various quasi-one-dimensional mixed-spin Heisenberg systems exhibiting ferrimagnetic ground states. Presented analysis of the asymptotic series up to second order in the parameter $1/S$ implies that in these systems the spin-wave interaction introduces numerically small corrections to the principal approximation, even in the extreme quantum limit $S = \frac{1}{2}$. Thus, indicated effectiveness of the spin-wave technique – as applied to magnetic systems with small spin quantum numbers and in restricted geometries – may be attributed to the observed weakness of spin-wave interactions.

The authors thank J. Richter and U. Schollwöck for their collaborations in this field, and S. Sachdev, A.W. Sandvik, and Z. Weihong for the permission to use their results. This work was supported by the Deutsche Forschungsgemeinschaft.

References

1. F. Bloch: Z. Physik **61**, 206 (1930)
2. F. Bloch: Z. Physik **74**, 295 (1932)
3. T. Holstein and H. Primakoff: Phys. Rev. **58**, 1098 (1940)
4. P.W. Anderson: Phys. Rev. **86**, 694 (1952)
5. R. Kubo: Phys. Rev. **87**, 568 (1952)
6. T. Oguchi: Phys. Rev. **117**, 117 (1960)
7. F. Dyson: Phys. Rev. **102**, 1217 (1956)
8. F. Dyson: Phys. Rev. **102**, 1230 (1956)
9. A.B. Harris, D. Kumar, B.I. Halperin, and P.C. Hohenberg: Phys. Rev. B **3**, 961 (1971)
10. S.V. Maleev: Sov. Phys. JETP **6**, 776 (1958)
11. S.V. Tyablikov: *Methods in the quantum theory of magnetism* (Plenum Press, New York 1967)
12. A.I. Akhiezer, V.G. Bar'yakhtar, and S.V. Peletminskii: *Spin waves* (John Wiley & Sons, New York 1968)
13. D.C. Mattis: *The Theory of Magnetism I: Statics and Dynamics* (Springer, Berlin Heidelberg 1981)

14. N.D. Mermin and H. Wagner: Phys. Rev. Lett. **22**, 1133 (1966)
15. E. Manousakis: Rev. Mod. Phys. **63**, 1 (1991)
16. N.B. Ivanov and U. Schollwöck: Quantum Heisenberg ferrimagnetic chains. In: *Contemporary Problems in Condensed Matter Physics*, ed by S.J. Vlaev, L.M. Gaggero Sager (Nova Science, New York 2001) pp. 145–181
17. C.M. Canali and S.M. Girvin: Phys. Rev. **45**, 7127 (1992)
18. O. Kahn, Y. Pei and Y. Journaux: Molecular Inorganic Magnetic Materials. In: *Inorganic Materials*, ed by D.W. Bruce, D. O'Hare (John Wiley & Sons, New York 1992)
19. M.I. Plumer, A. Caillé, A. Mailhot, and H.T. Diep: Critical Properties of Frustrated Vector Spin Models. In: *Magnetic Systems with Competing Interactions*, ed by H.T. Diep (World Scientific, Singapure 1994) pp. 1–50
20. E.F. Shender: Sov. Phys. JETP **56**, 178 (1982)
21. C.L. Henley: Phys. Rev. Lett. **62**, 2056 (1989)
22. E.H. Lieb and D.C. Mattis: J. Math. Phys. **3**, 749 (1962)
23. A. Auerbach: *Interacting Electrons and Quantum Magnetism* (Springer, New York Berlin 1998)
24. J. Schwinger: *Quantum Theory of Angular Momentum* (Academic Press, New York 1965)
25. J. Villain: J. Phys. (Paris) **35**, 27 (1974)
26. I. Goldhirsch, E. Levich, and V. Yachot: Phys. Rev. B **19**, 4780 (1979)
27. I. Goldhirsch: Phys. Rev. A **13**, 453 (1980)
28. J.H.P. Colpa: Physica A **93**, 327 (1978)
29. N.B. Ivanov: Phys. Rev. B **62**, 3271 (2000)
30. B.I. Halperin and P. C. Hohenberg: Phys. Rev. **188**, 898 (1969)
31. N.B. Ivanov and J. Richter: Phys. Rev. B **63**, 1444296 (2001)
32. N. Read and S. Sachdev: Phys. Rev. Lett. **75**, 3509 (1995)
33. S.K. Pati, S. Ramasesha and D. Sen: Phys. Rev. B **55**, 8894 (1997)
34. S. Brehmer, H.-J. Mikeska, and S. Yamamoto: J. Phys.: Condens. Matter **9**, 3921 (1997)
35. S. Yamamoto, S. Brehmer, and H.-J. Mikeska: Phys. Rev. B **57**, 13610 (1998)
36. C.J. Hamer, Z. Weihong, and P. Arndt: Phys. Rev. B **46**, 6276 (1992)
37. A.W. Sandvik: Phys. Rev. B **56**, 11678 (1997)
38. N.B. Ivanov: Phys. Rev. B **57**, R14024 (1998)
39. S.K. Pati, S. Ramasesha and D. Sen: J. Phys.: Condens. Matter **9**, 8707 (1997)
40. L. Hulthen: Ark. Met. Astron. Fysik A **26**, Na. 11 (1938)
41. K. Hallberg, X.Q.G. Wang, P. Horsch, and A. Moreo: Phys. Rev. Lett. **76**, 4955 (1996)
42. I. Affleck, D. Gepner, H.J. Schulz, and T. Ziman: J. Phys. A **22**, 511 (1989)
43. J. Des Cloizeaux and J.J. Pearson: Phys. Rev. **128**, 2131 (1962)
44. I. Affleck: J. Phys.: Condens. Matter **1**, 3047 (1989)
45. G. Baym and A.M. Sessler: Phys. Rev. **131**, 2345 (1963)
46. P. Kopietz: Phys. Rev. B **41**, 9228 (1990)
47. T. Ono, T. Nishimura, M. Katsumura, T. Morita, and M. Sugimoto: J. Phys. Soc. Jpn. **66**, 2576 (1997)
48. S. Chakravarty, B.I. Halperin, and D.R. Nelson: Phys. Rev. B **39**, 9228 (1990)
49. P. Hasenfratz and F. Niedermayer: Z. Phys. B **92**, 91 (1993)
50. A.V. Chubukov, S. Sachdev, and J. Ye: Phys. Rev. B **49**, 11919 (1994)

51. I. Affleck: Field theory methods and quantum critical phenomena. In: *Fields, Strings and Critical Phenomena*, ed by E. Brézin, J. Zinn-Justin (North-Holland, Amsterdam 1989) pp. 563–640
52. E. Fradkin: *Field Theories of Condensed Matter Systems* (Addison-Wesley, Redwood City 1991)
53. S. Sachdev: *Qantum Phase Transitions* (Cambridge Univ. Press, New York 1999)
54. J.D. Reger and A.P. Young: Phys. Rev. B **37**, 5978 (1988)
55. R.R.P. Singh: Phys. Rev. B **39**, 9760 (1989)
56. R.R.P. Singh and D.A. Huse: Phys. Rev. B **40**, 7247 (1989)
57. Z. Weihong, J. Oitmaa, and C.J. Hamer: Phys. Rev. B **43**, 8321 (1991)
58. C.M. Canali, S.M. Girvin, and M. Wallin: Phys. Rev. B **45**, 10131 (1992)
59. J. Igarashi: Phys. Rev. B **46**, 10763 (1992)
60. Z. Weihong and C.J. Hamer: Phys. Rev. B **47**, 7961 (1993)
61. C.J. Hamer, Z. Weihong, and J. Oitmaa: Phys. Rev. B **50**, 6877 (1994)
62. W.H. Zheng, J. Oitmaa, and C.J. Hamer: Phys. Rev. B **43**, 8321 (1991
63. C. Lhuillier and G. Misguich: Frustrated quantum magnets. In: Lecture Notes in Physics 595, *H*igh magnetic fields, ed by C. Berthier, L.P. Lévy, G. Martinez (Springer, Berlin 2001) pp. 161–190
64. B. Bernu, P. Lecheminant, C. Lhuillier, and L. Pierre: Phys. Rev. B **50**, 10048 (1994)
65. A.V. Chubukov, S. Sachdev, and T. Senthil: J. Phys. Condens. Matter **6**, 8891 (1994)
66. Th. Jolicoeur and J. C. Le Guillou: Phys. Rev. B **40**, 2727 (1989)
67. T. Dombre and N. Read: Phys. Rev. B **39**, 6797 (1989)
68. S.J. Miyake: J. Phys. Soc. Jpn. **61**, 983 (1992)
69. L. Capriotti, A.E. Trumper, and S. Sorella: Phys. Rev. Lett. **82**, 3899 (1999)
70. A.V. Chubukov: Phys. Rev. B **44**, 5362 (1991)
71. A.V. Chubukov and D.I. Golosov: J. Phys.: Condens. Matter **3**, 69 (1991)
72. A.E. Trumper, L. Capriotti, and S. Sorella: Phys. Rev. B **61**, 11529 (2000)
73. A.F. Andreev and V.I. Marchenko: Sov. Phys. Usp. **23**, 21 (1980)
74. M. Takahashi: Prog. Theor. Phys. **87**, 233 (1986)
75. M. Takahashi: Phys. Rev. Lett. **58**, 168 (1987)
76. J.E. Hirsch and S. Tang: Phys. Rev. B **40**, 4769 (1989)
77. Q.F. Zhong and S. Sorella: Europhys. Lett. **21**, 629 (1993)
78. M. Takahashi: Phys. Rev. B **40**, 2494 (1989)
79. D.P. Arovas and A. Auerbach: Phys. Rev. B **38**, 316 (1988)
80. A.V. Dotsenko and O.P. Sushkov: Phys. Rev. B **50**, 13821 (1994)
81. A.M. Tsvelik: *Quantum Field Theory in Condensed Matter Physics* (Cambridge Univ. Press, Cambridge 1995)
82. P. Hasenfratz, M. Maggiore, and F. Niedermayer: Phys. Lett. B **245**, 522 (1990)
83. H. Neuberger and T. Ziman: Phys. Rev. B **39**, 2608 (1989)
84. D.S. Fisher: Phys. Rev. B **39**, 11783 (1989)
85. F.D.M. Haldane: Phys. Rev. Lett. **50**, 1153 (1983)
86. F.D.M. Haldane: Phys. Lett. A **93**, 464 (1983)